Constructing hydrogen bond based melam/WO3 heterojunction with enhanced visible-light photocatalytic activity

doi: info:doi/10.1016/j.apcatb.2016.12.069

Electronic Supplementary Information

Constructing hydrogen bond based melam/WO_3 heterojunction with enhanced visible-light photocatalytic activity

Zhengyuan Jin,[a,b] Qitao Zhang,[b] Liang Hu,[a] Jiaqi Chen,[a] Xing Cheng,[c] Yu-Jia Zeng, [a,d,*] Shuangchen Ruan,[a,**] and Teruhisa Ohno[b]

[a] Shenzhen Key Laboratory of Laser Engineering, College of Optoelectronic Engineering, Shenzhen University, Shenzhen, 518060, P. R. China

[b] Department of Applied Chemistry, Faculty of Engineering, Kyushu Institute of Technology, 1-1 Sensuicho, Tobata, Kitakyushu 804-8550, Japan

[c] Department of Materials Science and Engineering, South University of Science and Technology of China (SUSTC)

[d] State Key Laboratory of Silicon Materials, Department of Materials Science and Engineering, Zhejiang University, Hangzhou 310027, P. R. China.

Table of contents

SUPPORTING DATA

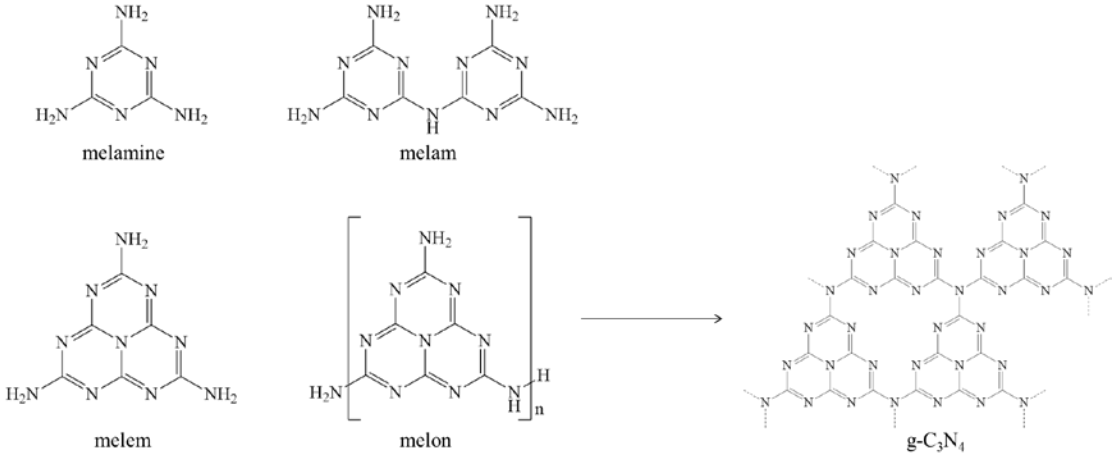

Scheme S1 The structures of the carbon nitride family, such as melamine, melam, melem, melon, and g-C_3N_4. Scheme adapted from Lau et al [1].

Figure data

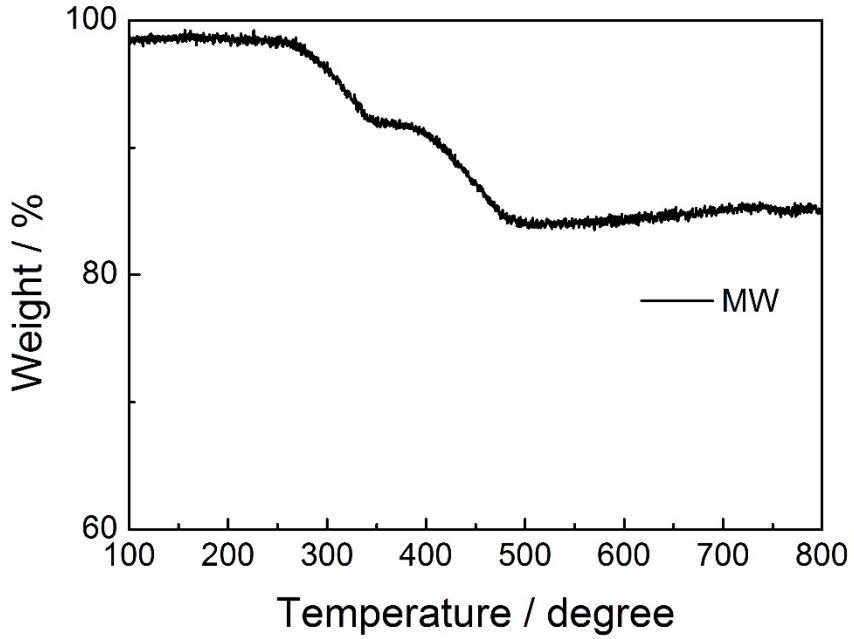

Figure S1 TG analysis of MW (10 mg) between 100 ^{o}C and 800 ^{o}C at a heating rate of 10 ^{o}C min^{-1}.

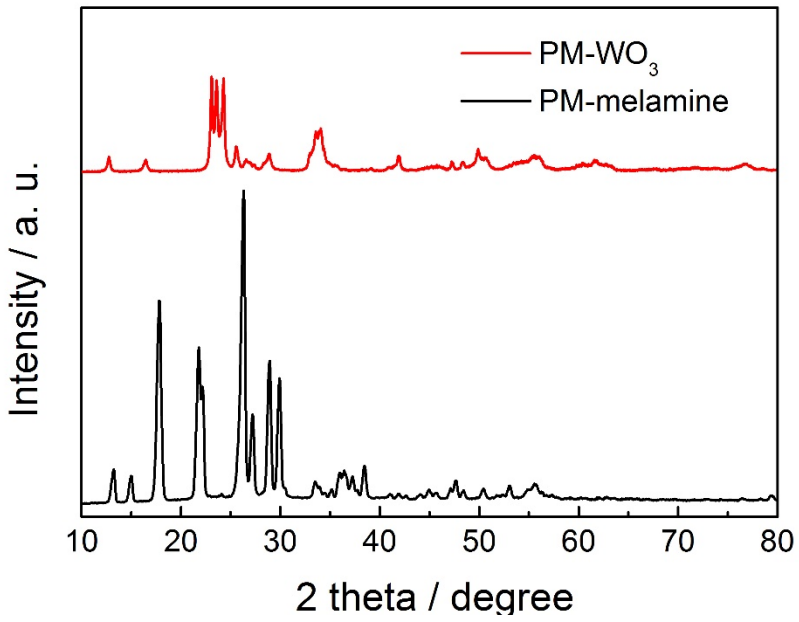

Figure S2 XRD patterns of melamine and WO_3 after planetary milling treatment.

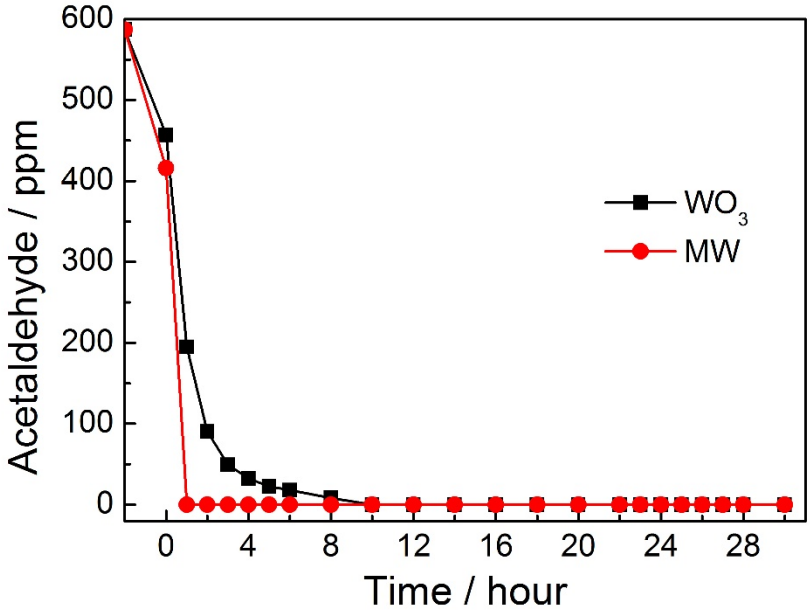

Figure S3 Time courses of acetaldehyde from acetaldehyde photodecomposition.

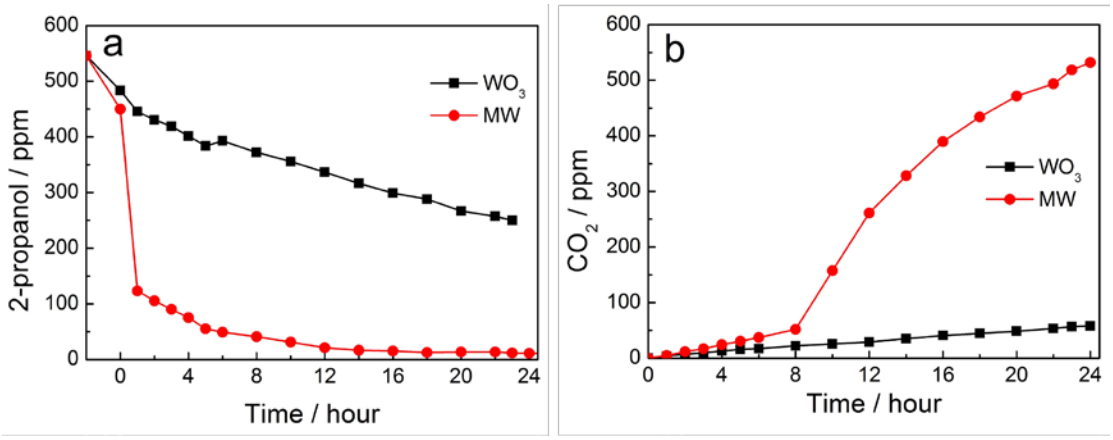

Figure S4 Time courses of 2-propanol (a) and CO_2 (b) from 2-propanol photodecomposition.

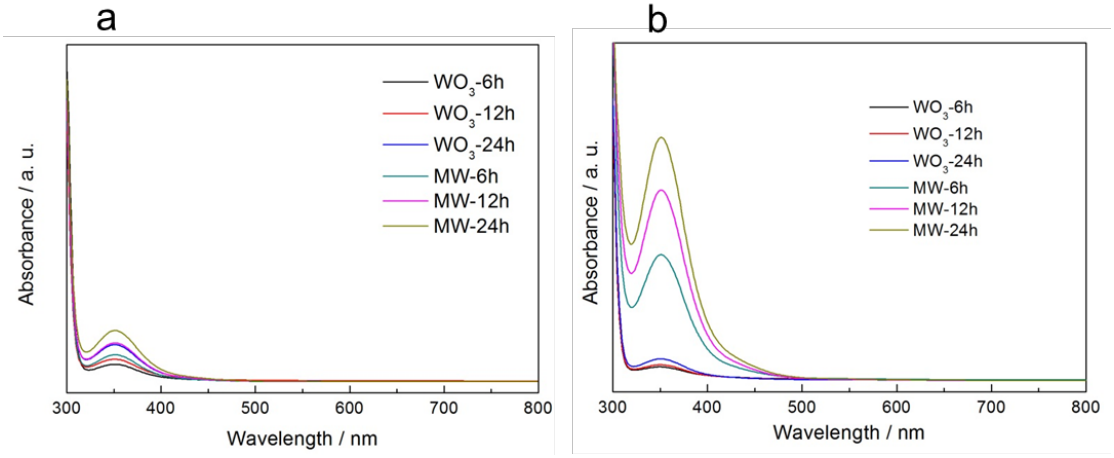

Figure S5 UV-vis absorption spectrum changes of H_2O_2 generation in acetic acid solution and pure H_2O under visible light irradiation (435 nm, 3 mW cm^{-2}).

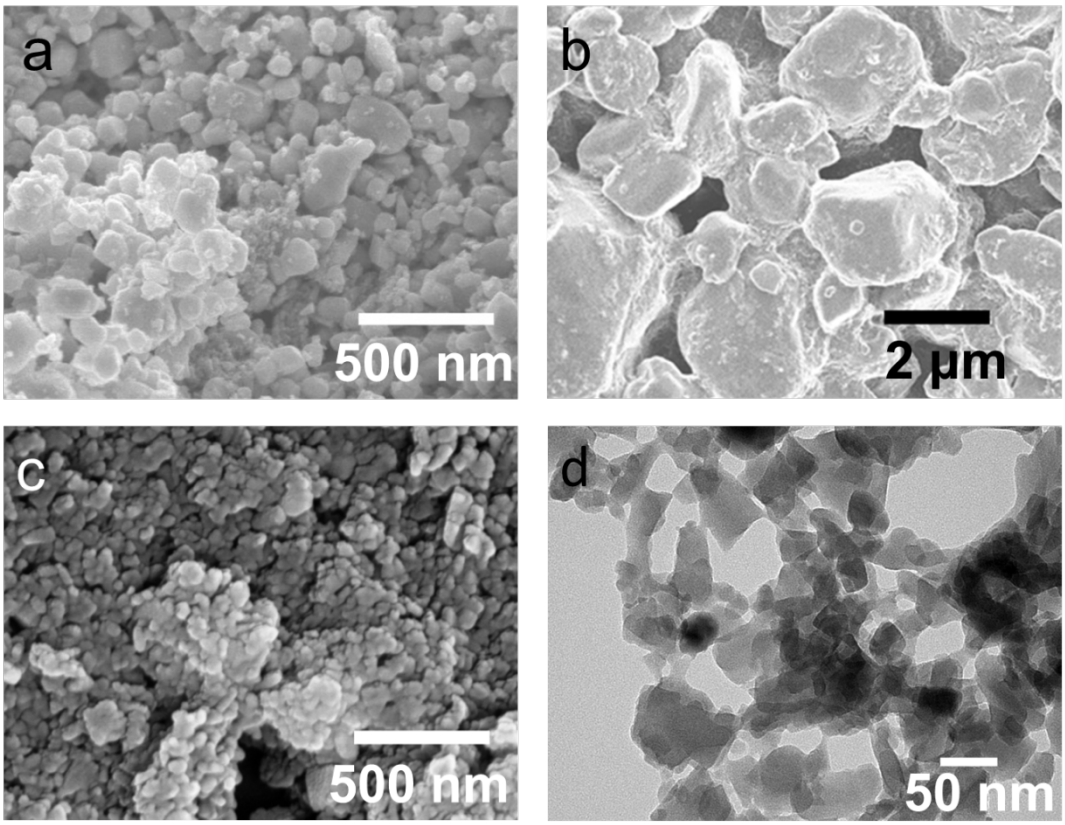

Figure S6 SEM images of WO_3 (a), melamine (b), and MW (c); (d) TEM image of MW.

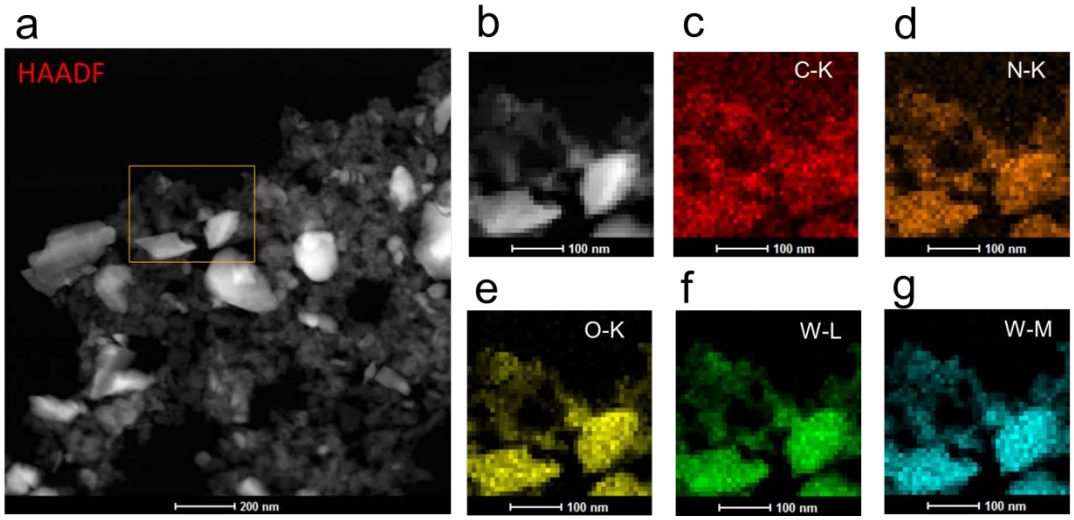

Figure S7 HAADF-STEM and EDS mapping images of MW.

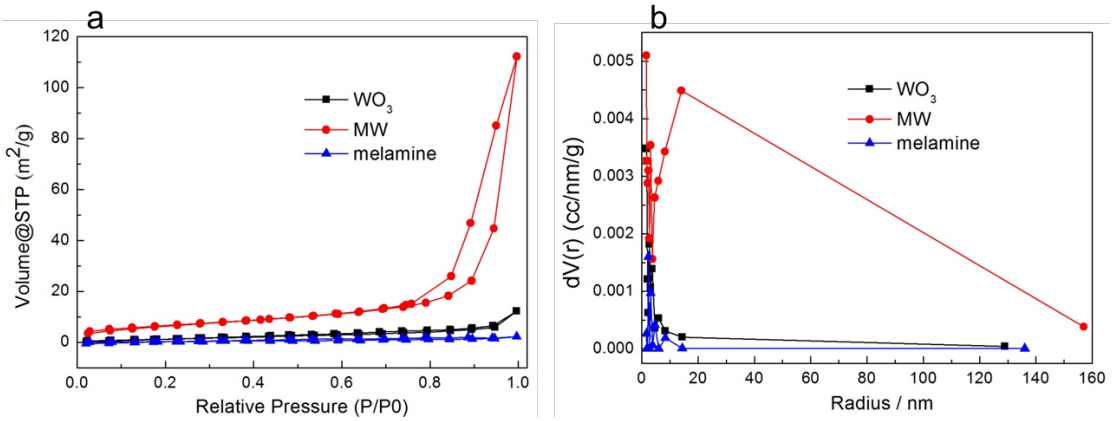

Figure S8 (a) BET N_2 adsorption isotherms and (b) BJH pore size distributions of WO_3, melamine, and MW.

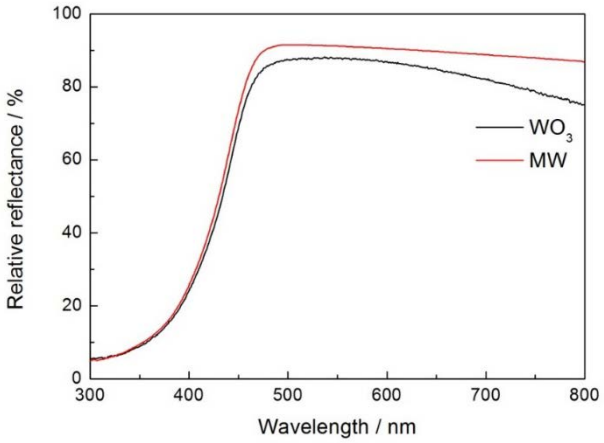

Figure S9 UV-vis diffuse reflectance spectra of WO_3 and MW.

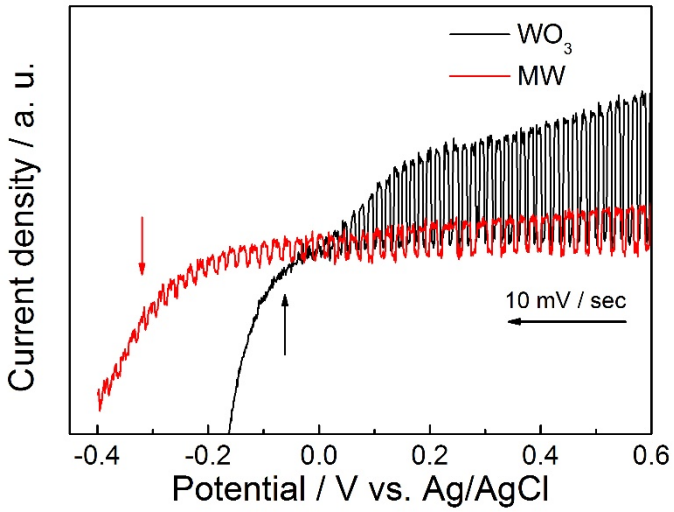

Figure S10 Linear sweep voltammetry of WO_3 and MW electrodes.

Figure S11 The WO_3 and MW fabricated onto electrode on a FTO by electrophoresis method.

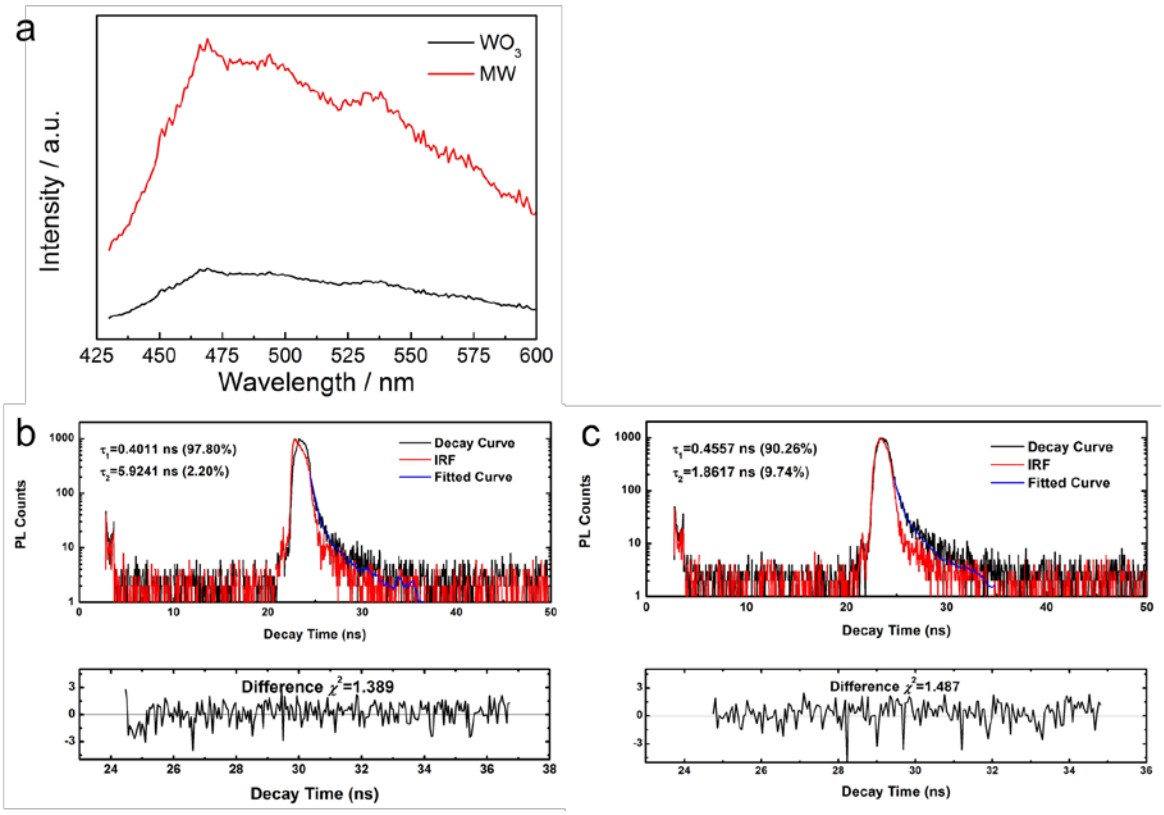

Figure S12 (a) Photoluminescence spectra of samples, the time-resolved fluorescence decay spectra of (b) WO_3 and (c) MW.

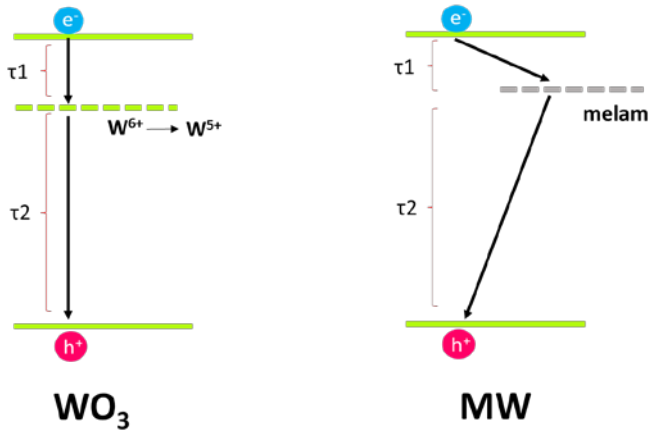

Figure S13 The behavior of photo-exited charge carriers [2-3].

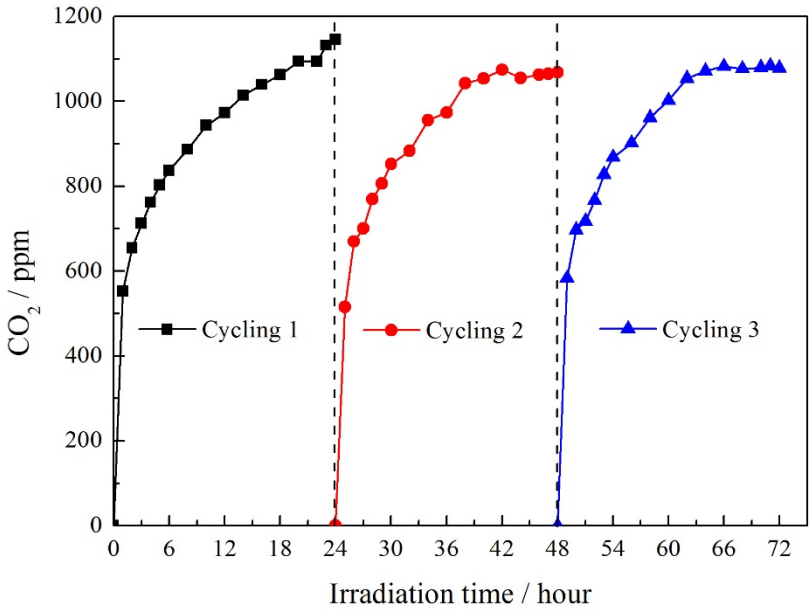

Figure S14 The photocatalytic activity results of acetaldehyde degradation. Three-cycle test by MW.

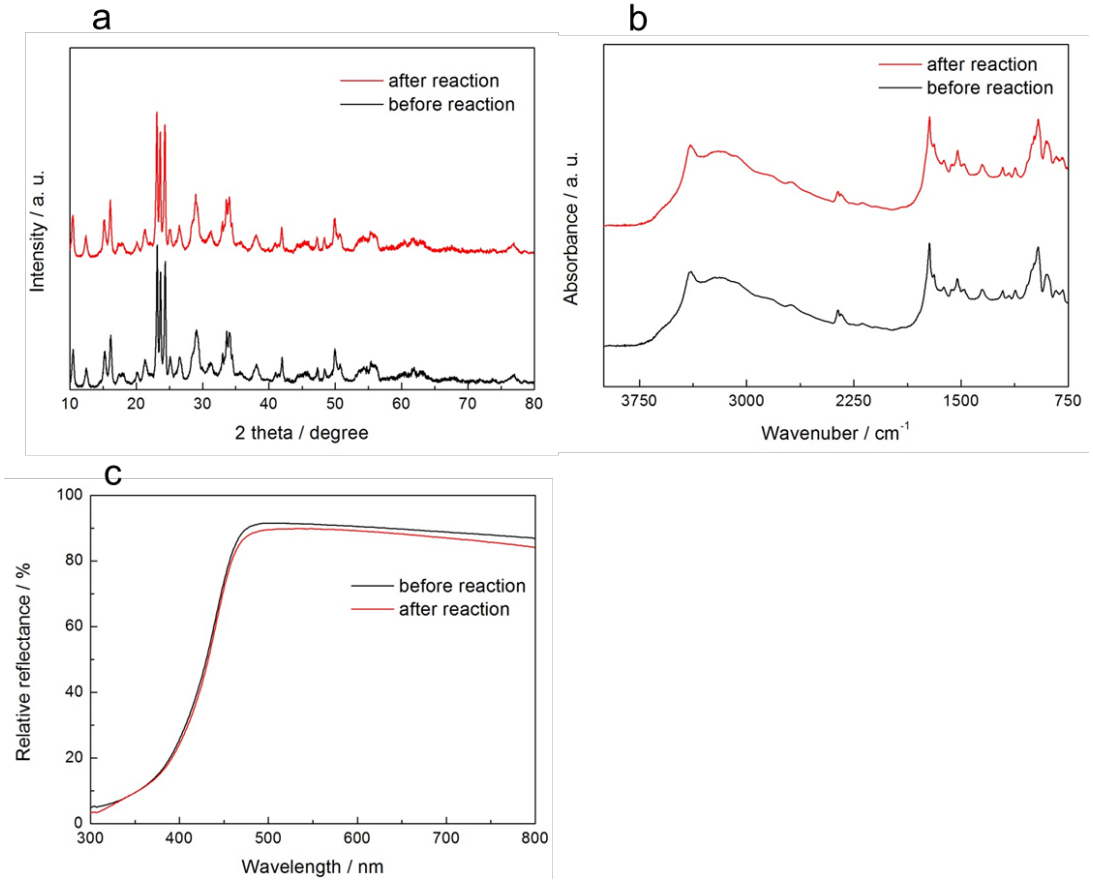

Figure S15 (a) XRD, (b) FTIR, and (c) UV-vis DRS of MW before and after photocatalytic reaction.

Reference

[1] A. van Dijken, E.A. Meulenkamp, D. Vanmaekelbergh, A. Meijerink, J. Phys. Chem. B, 104 (2000) 1715-1723.

[2] L. Hu, J. Huang, H. He, L. Zhu, S. Liu, Y. Jin, L. Sun, Z. Ye, Nanoscale, 5 (2013) 3918-3930.

[3] B.V. Lotsch, M. Döblinger, J. Sehnert, L. Seyfarth, J. Senker, O. Oeckler, W. Schnick, Chem. Eur. J. 13 (2007) 4969-4980.